

MPI-Ph/97-015
TUM-HEP-274/97

DESY 97-119
hep-ph/9706501

Penguin Diagrams, Charmless B-Decays and the “Missing Charm Puzzle”¹

Alexander Lenz²,

Max-Planck-Institut für Physik — Werner-Heisenberg-Institut,
Föhringer Ring 6, D-80805 München, Germany,

Ulrich Nierste³,

DESY - Theory group, Notkestrasse 85, D-22607 Hamburg, Germany,

and

Gaby Ostermaier⁴

Physik-Department, TU München, D-85747 Garching, Germany

Abstract

We calculate the contributions of penguin diagrams with internal u or c quarks to various inclusive charmless B-decay rates. Further we analyze the influence of the chromomagnetic dipole operator Q_8 on these rates. We find that the rates corresponding to $\bar{B} \rightarrow X_{u\bar{u}s}$, $\bar{B} \rightarrow X_{d\bar{d}s}$, $\bar{B} \rightarrow X_{s\bar{s}s}$, $\bar{B} \rightarrow X_{s\bar{s}d}$ and $\bar{B} \rightarrow X_{d\bar{d}d}$ are dominated by the new penguin contributions. The contributions of Q_8 sizably diminish these rates. Despite of an increase of the total charmless decay rate by 36 % the new contributions are not large enough to explain the charm deficit observed by ARGUS and CLEO. We predict $n_c = 1.33 \pm 0.06$ for the average number of charmed particles per B-decay in the Standard Model. Then the hypothesis of an enhancement of the chromomagnetic dipole coefficient C_8 by new physics contributions is analyzed. We perform a model independent fit of C_8 to the experimental data. If the CKM structure of the new physics contribution is the same as in the Standard Model, $|C_8(M_W)|$ must be enhanced by a factor of 9 to 16 in order to explain the observed charm deficit.

¹Work supported by BMBF under contract no. 06-TM-874.

²e-mail:alenz@MPPMU.MPG.DE

³e-mail:nierste@mail.desy.de

⁴e-mail:Gaby.Ostermaier@feynman.t30.physik.tu-muenchen.de

1. Introduction

Precision measurements performed at the $\Upsilon(4S)$ resonance find less charmed particles in the final states of B meson decays than theoretically expected. The CLEO 1.5, CLEO II and ARGUS data give [1]

$$n_c^{exp} = 1.15 \pm 0.05 \quad (1)$$

for the average number of charm (anti-)quarks per B^+/B^0 -decay. Complementary information on inclusive B decays can be obtained from the semileptonic branching ratio. The CLEO and ARGUS groups [1, 2] have measured

$$B_{SL}^{exp} = 10.23 \pm 0.39\%. \quad (2)$$

The increasing experimental precision achieved in the current decade has been paralleled by a substantial progress in the theoretical understanding of the inclusive decay rates entering B_{SL} and n_c . Here the calculational key is the heavy quark expansion (HQE) [3, 4] of the decay rate in question: The leading term of the HQE reproduces the decay rate of a b-quark in the QCD-corrected parton model. The first non-perturbative corrections are suppressed by a factor of $(\Lambda_{QCD}/m_b)^2$ and affect the rates by at most a few percent. Theoretically spectator effects of order $16\pi^2(\Lambda_{QCD}/m_b)^3$ [5, 6] could be larger [6], but for the decay rates of B^\pm and B^0 entering (2) and (1) they are experimentally known to be at the percent level as well [7]. The apparent smallness of these non-perturbative terms has shifted the focus towards the perturbative corrections to the free quark decay. The calculation of such short distance effects starts from an effective hamiltonian, whose generic form reads

$$H = \frac{G_F}{\sqrt{2}} \left[V_{CKM} \sum_{j=1}^2 C_j Q_j - V'_{CKM} \left(\sum_{k=3}^6 C_j Q_j + C_8 Q_8 \right) \right]. \quad (3)$$

Here G_F is the Fermi constant and V_{CKM} and V'_{CKM} are products of elements of the Cabibbo-Kobayashi-Maskawa (CKM) matrix. The Wilson coefficients C_j encode the physics connected to the weak scale and play the rôle of effective coupling constants of the local interactions described by the operators Q_j . Their precise form depends on the flavour structure of the decay and will be given below in (13).

Decays with three different flavours in the final state such as $b \rightarrow c\bar{u}d$ can only proceed through the current-current operators Q_1 and Q_2 . $\Gamma(b \rightarrow c\bar{u}d)$ has been calculated to order α_s , which is the next-to-leading order (NLO), in [8]. The generic Feynman diagram for these corrections are depicted in Fig. 1. In [9] the same diagrams have been calculated for $\Gamma(b \rightarrow c\bar{c}s) + \Gamma(b \rightarrow c\bar{c}d)$. The latter decays and the charmless nonleptonic decays, however, also involve penguin effects. Diagrams with insertions of the penguin operators Q_{3-6} have been taken into account only in the leading order (LO) [9–11], because their coefficients C_{3-6} are much smaller than $C_{1,2}$ (cf. Tab. 1). The results for B_{SL} and n_c read

$$B_{SL} = (11.7 \pm 1.4 \pm 1.0)\%, \quad n_c = 1.34 \mp 0.06. \quad (4)$$

Here the result for B_{SL} has been obtained in [10, 12] with the analytical input from [8–10]. The second error bar has been added to account for the spectator effects estimated in [6]. Apparently

there is no spectacular discrepancy between (2) and (4). The result for n_c in (4) does not involve the calculation of $\Gamma(b \rightarrow c\bar{c}d) + \Gamma(b \rightarrow c\bar{c}s)$, but instead uses the experimental information on B_{SL} in (2) as proposed in [13, 14]. We discuss this in more detail in sect. 2.

The discrepancy between (1) and (4) constitutes the “missing charm puzzle”. The search for a theoretical explanation has recently focused on new positive contributions to the yet unmeasured charmless decay modes entering (4). Indeed, in a recent analysis [14] $\Gamma(b \rightarrow \text{no charm})$ has been estimated indirectly in two different ways: First the experimental information on final states with hadrons containing a c quark has been used and second data on decay products involving a \bar{c} quark have been analyzed. For the CLEO data both methods consistently indicate an enhancement of $\Gamma(b \rightarrow \text{no charm})$ by roughly a factor of 14 compared to the theoretical prediction in [11].

Next we briefly discuss the LEP results for B_{SL} and n_c [15]. The LEP Z-peak experiments encounter a mixture of b-flavoured hadrons. In order to allow for a comparison with (2) one must correct the LEP result $B_{SL}^{Z,\text{exp}} = 10.95 \pm 0.42\%$ [1] for the different lifetimes [7] of the hadrons in the mixture [16]:

$$B_{SL}^{Z,\text{corr,exp}} = 11.13 \pm 0.42\%, \quad n_c^{Z,\text{exp}} = 1.22 \pm 0.08. \quad (5)$$

These data are consistent with the theory (cf. (9) below), but the analysis in [14] has found evidence for an enhanced $\Gamma(b \rightarrow \text{no charm})$ also from the LEP data. Further the two methods used in [14] have given less consistent results for the LEP data than for the CLEO data. In addition the LEP measurements involve the Λ_b baryon, whose lifetime is either not properly understood theoretically or incorrectly measured. (If the latter is the case, $B_{SL}^{Z,\text{corr,exp}}$ in (5) must be replaced by the uncorrected $B_{SL}^{Z,\text{exp}}$, which reduces the 2σ discrepancy between (2) and (5).) Hence in our analysis we will mainly use (2) and (1).

Now two possible sources of an enhanced $\Gamma(b \rightarrow \text{no charm})$ are currently discussed: The authors of [17] stress the possibility that the Wilson coefficient C_8 of the chromomagnetic dipole operator Q_8 is enhanced by new physics contributions. On the other hand in [14, 18] an explanation within QCD dynamics is suggested: An originally produced (c, \bar{c}) -pair can annihilate and thereby lead to a charmless final state.

The calculation of matrix elements involving Q_{3-6} and Q_8 does not exhaust all possible penguin effects. In this paper we calculate the contributions of penguin diagrams with insertions of the current-current operator Q_2 to the decay rates into charmless final states (see Fig. 2). Such a penguin diagram with a (c, \bar{c}) -pair in the intermediate state involves the large coefficient C_2 and the CKM factor $V_{cb} \gg |V_{ub}|$. It is precisely the short distance analogue of the mechanism proposed in [14, 18] and surprisingly has not been considered in the perturbative calculations [9–11, 20] of the decay rates entering B_{SL} and n_c .

Further we calculate the diagrams involving the interference of the tree diagram with Q_8 in Fig. 3 with Q_{1-6} , which belongs to the order α_s as well. The consideration of these diagrams is mandatory, if one wants to estimate the effect of an enhanced coefficient C_8 on $\Gamma(b \rightarrow \text{no charm})$ proposed in [17].

The paper is organized as follows: In the following section we set up our notations and collect results from earlier work. The calculation of the penguin diagram contributions and the $Q_{1-6}-Q_8$

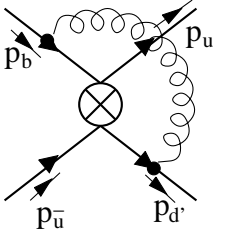


Figure 1: Example of a current-current diagram. The cross denotes the inserted operator. d' equals d or s .

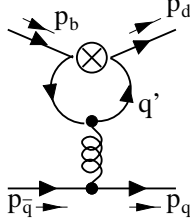


Figure 2: Penguin diagram involving Q_2 . The internal quark q' can be u or c . The corresponding diagram with Q_1 vanishes.

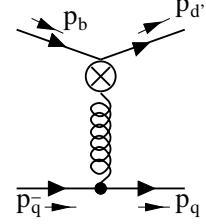


Figure 3: Tree diagram contribution of Q_8 to $\Gamma(b \rightarrow q\bar{q}d')$.

interference terms is presented in sect. 3. The phenomenologically interested reader is referred to sect. 4, in which we discuss our numerical results. In sect. 4 we also comment on the mechanism proposed in [18]. Further a potential enhancement of C_8 is analyzed by a model independent fit of C_8 to the experimental data. Finally we conclude.

2. Preliminaries

2.1. B_{SL} and n_c

For the theoretical description of the various decay rates it is advantageous to normalize them to the well-understood semileptonic decay rate [13, 14]:

$$r_{q\ell} = \frac{\Gamma(\overline{B} \rightarrow X_q \ell \bar{\nu}_\ell)}{\Gamma(\overline{B} \rightarrow X_c e \bar{\nu}_e)}, \quad r_{q_1 \bar{q}_2 q_3} = \frac{\Gamma(\overline{B} \rightarrow X_{q_1 \bar{q}_2 q_3})}{\Gamma(\overline{B} \rightarrow X_c e \bar{\nu}_e)}, \quad r_{qg} = \frac{\Gamma(\overline{B} \rightarrow X_{qg})}{\Gamma(\overline{B} \rightarrow X_c e \bar{\nu}_e)}. \quad (6)$$

This eliminates the factor of m_b^5 common to all decay rates. For the charmless decays we will further use

$$r_\phi = \sum_{\substack{q=d,s \\ q'=u,d,s}} [r_{q' \bar{q}' q} + r_{qg}] + 2r_{ue}. \quad (7)$$

The semileptonic branching ratio reads

$$B_{SL} = \frac{1}{2 + r_{c\tau} + r_\phi + \sum_{q=d,s} [r_{c\bar{u}q} + r_{c\bar{c}q}]}.$$

Small contributions such as $r_{u\tau} = 0.004$ and radiative decay modes have been omitted in (7). In (8) also $r_{u\bar{c}s} = 0.05$ [11] has been neglected. The numerical value for B_{SL} in (4) is the average of the two results given in [10] corresponding to two different renormalization schemes (on-shell

vs. $\overline{\text{MS}}$ [21] quark masses). In the corresponding expression for n_c the term $r_{c\bar{c}s} + r_{c\bar{c}d}$, which suffers from sizeable theoretical uncertainties, is eliminated in favour of B_{SL} [13, 14]:

$$n_c = 2 - (2 + r_{c\tau} + r_{c\bar{u}d} + r_{c\bar{u}s} + 2r_\phi) B_{SL}. \quad (9)$$

Yet with [8, 22]

$$r_{c\bar{u}s} + r_{c\bar{u}d} = 4.0 \pm 0.4, \quad r_{c\tau} = 0.25 \quad (10)$$

and B_{SL}^{exp} in (2) one obtains

$$n_c = 1.36 \mp 0.04 - 0.205 \cdot r_\phi. \quad (11)$$

Now the current-current type radiative corrections to r_ϕ (cf. Fig. 1) have been calculated in [8, 20, 23] using different renormalization schemes. The penguin operators Q_{3-6} have been included within the LO in [11]. With up-to-date values for B_{SL} and the CKM elements the calculation of [11] yields $r_\phi = 0.11 \pm 0.08$. Inserting this result into (11) yields the numerical value in (4). In contrast the indirect experimental determination in [14] has found $r_\phi = 1.6 \pm 0.4$. In order to reproduce the experimental value of n_c in (1) one needs $r_\phi = 1.0 \pm 0.4$.

So far the penguin diagrams of Fig. 2 have not been calculated for all possible charmless B decay modes. Yet for the pure penguin induced decays of a b -quark into three down-type (anti)-quarks the contribution of the diagram of Fig. 2 has been obtained in terms of a twofold integral representation in [19]. Likewise the effect of penguin diagrams on the analysis of CP asymmetries has been studied in [19, 24] and in [25] penguin effects on exclusive decays have been studied.

2.2. Decay rates to order α_s

In order to describe decays of the type $b \rightarrow q\bar{q}d$ one needs the following hamiltonian:

$$H = \frac{G_F}{\sqrt{2}} \left\{ \sum_{j=1}^2 C_j \left(\xi_c^* Q_j^c + \xi_u^* Q_j^u \right) - \xi_t^* \sum_{j \in \mathcal{P}} C_j Q_j \right\}, \quad \xi_{q'} = V_{q'b}^* V_{q'd}. \quad (12)$$

Here $\xi_u + \xi_c + \xi_t = 0$ due to the unitarity of the CKM matrix and $\mathcal{P} = \{3, \dots, 6, 8\}$. H in (12) comprises the following operator basis:⁵

$$\begin{aligned} Q_1^q &= (\bar{d}q)_{V-A} \cdot (\bar{q}b)_{V-A} \cdot \tilde{\mathbb{1}} \\ Q_2^q &= (\bar{d}q)_{V-A} \cdot (\bar{q}b)_{V-A} \cdot \mathbb{1} \\ Q_3^q &= (\bar{d}b)_{V-A} \cdot (\bar{q}q)_{V-A} \cdot \mathbb{1}, & Q_4^q &= (\bar{d}b)_{V-A} \cdot (\bar{q}q)_{V-A} \cdot \tilde{\mathbb{1}} \\ Q_5^q &= (\bar{d}b)_{V-A} \cdot (\bar{q}q)_{V+A} \cdot \mathbb{1}, & Q_6^q &= (\bar{d}b)_{V-A} \cdot (\bar{q}q)_{V+A} \cdot \tilde{\mathbb{1}} \\ Q_j &= \sum_{q=u,d,s,c,b} Q_j^q & \text{for } 3 \leq j \leq 6, \\ Q_8 &= -\frac{g}{8\pi^2} \bar{d}\sigma^{\mu\nu} [m_d L + m_b R] T^a b \cdot G_{\mu\nu}^a. \end{aligned} \quad (13)$$

⁵The overall sign of the matrix element $\langle Q_8 \rangle$ depends on the chosen sign of the coupling g in the covariant derivative in the QCD lagrangian. The definition in (13) complies with the result in [26, 27], if the covariant derivative is chosen as $D_\mu = \partial_\mu - igT^a A_\mu^a$, so that the Feynman rule for the fermion-gluon vertex is igT^a . By convention the notation Q_7 is reserved for the magnetic $\bar{d}b\gamma$ -operator, which we do not need in our calculation.

The colour singlet and non-singlet structure are indicated by $\mathbb{1}$ and $\tilde{\mathbb{1}}$ and $V \pm A$ is the Dirac structure, i.e.

$$(\bar{d}q)_{V-A} \cdot (\bar{q}b)_{V-A} \cdot \tilde{\mathbb{1}} = \bar{d}_\alpha \gamma_\mu (1 - \gamma_5) q_\beta \cdot \bar{q}_\beta \gamma^\mu (1 - \gamma_5) b_\alpha.$$

Next it is useful to expand the renormalized matrix elements in α_s and to separate the result from current-current diagrams (see Fig. 1) and penguin diagrams (see Fig. 2):

$$\langle q\bar{q}d | Q_j^{q'} | b \rangle = \langle Q_j^{q'} \rangle^{(0)} + \frac{\alpha_s}{4\pi} \left[\langle Q_j^{q'} \rangle_{cc}^{(1)} + \langle Q_j^{q'} \rangle_{peng}^{(1)} \right] + O(\alpha_s^2), \quad j = 1, 2, \quad (14)$$

$$\langle Q_j^{q'} \rangle_{peng}^{(1)} = \sum_{k \in \mathcal{P}} r_{jk}^{q'} (p^2, m_{q'}, \mu) \langle Q_k \rangle^{(0)}, \quad p = p_b - p_d. \quad (15)$$

Of course $\langle Q_j^{q'} \rangle^{(0)}$ and $\langle Q_j^{q'} \rangle_{cc}^{(1)}$ are non-zero only for $q = q' = u$, recall that we do not consider $q = c$ in this work. In (15) we have expressed the result of the penguin diagram in terms of the tree-level matrix elements. There μ is the renormalization scale. For the momentum flow cf. Fig. 2.

The quark decay rate is related to the matrix element of H via

$$\Gamma(b \rightarrow q\bar{q}d) = \frac{1}{2m_b} \int \frac{d^3 \vec{p}_q d^3 \vec{p}_{\bar{q}} d^3 \vec{p}_d}{(2\pi)^5 8 |E_q E_{\bar{q}} E_d|} \delta^{(4)}(p_b + p_{\bar{q}} - p_q - p_d) \overline{\langle q\bar{q}d | H | b \rangle} \langle q\bar{q}d | H | b \rangle^*.$$

The bar over $\langle q\bar{q}d | H | b \rangle$ $\langle q\bar{q}d | H | b \rangle^*$ denotes the average over initial state polarizations and the sum over final state polarizations. Next we expand the decay rate to order α_s :

$$\Gamma(b \rightarrow q\bar{q}d) = \Gamma^{(0)} + \frac{\alpha_s(\mu)}{4\pi} [\Delta\Gamma_{cc} + \Delta\Gamma_{peng} + \Delta\Gamma_8 + \Delta\Gamma_W] + O(\alpha_s^2). \quad (16)$$

For $b \rightarrow q\bar{q}s$ decays one simply substitutes d by s in (13-16). Now the first two terms of the NLO correction in (16) describe the effect of current-current and penguin diagrams involving Q_1 or Q_2 . $\Delta\Gamma_8$ likewise contains the matrix elements of Q_8 . The remaining part $\Delta\Gamma_W$ of the NLO contribution is made of the corrections to the Wilson coefficients [20, 28] multiplying the tree-level amplitudes in $\Gamma^{(0)}$. We write

$$C_j(\mu) = C_j^{(0)}(\mu) + \frac{\alpha_s(\mu)}{4\pi} \Delta C_j(\mu), \quad j = 1, \dots, 6. \quad (17)$$

Here ΔC_j is the NLO correction to the Wilson coefficient. ΔC_j depends on the renormalization scheme chosen. This scheme dependence cancels with a corresponding one in the results of the loop diagrams contained in $\Delta\Gamma_{cc}$ and $\Delta\Gamma_{peng}$. For example the scheme dependence of $\Delta C_{1,2}$ cancels in combination with the current-current type corrections to Q_1 and Q_2 of Fig. 1. Since we do not include the unknown radiative corrections to the penguin operators Q_{3-6} in (16), we must likewise leave out terms in ΔC_j related to the NLO penguin-penguin mixing in order to render Γ in (16) scheme independent. We ban these technical details into the appendix. The values of the Wilson coefficients needed for the numerical evaluation of the various decay rates are listed in Tab. 1.

j	1	2	3	4	5	6	8
$C_j^{(0)}(\mu = m_b)$	-0.2493	1.1077	0.0111	-0.0256	0.0075	-0.0315	-0.1495
$C_j^{NDR}(\mu = m_b)$	-0.1739	1.0731	0.0113	-0.0326	0.0110	-0.0384	
$C_j^{(0)}(\mu = m_b/2)$	-0.3611	1.1694	0.0170	-0.0359	0.0100	-0.0484	-0.1663
$C_j^{NDR}(\mu = m_b/2)$	-0.2720	1.1246	0.0174	-0.0461	0.0149	-0.0587	
$C_j^{(0)}(\mu = 2m_b)$	-0.1669	1.0671	0.0071	-0.0176	0.0054	-0.0202	-0.1355
$C_j^{NDR}(\mu = 2m_b)$	-0.1001	1.0389	0.0073	-0.0227	0.0079	-0.0251	
$\Delta \bar{C}_j(\mu = m_b)$	2.719	-1.744	0.380	-0.1050	-0.223	0.384	

Table 1: Wilson coefficients used in our analysis. $C_j^{(0)}$ is the LO expression, C_j^{NDR} is the NLO coefficient in the NDR scheme. In C_j^{NDR} above the NLO corrections to penguin-penguin mixing have been omitted in order to render Γ in (28) scheme independent as described in the text. For $\mu = m_b$ this affects C_3 and C_5 by 12 % and 25 %, but is negligible for the other coefficients. $C_j^{(0)}$ and C_j^{NDR} are needed for the numerical evaluation of the decay rate in (28). $\Delta \bar{C}_j$ in the last line is defined in (42). The top and bottom mass are chosen as $m_t = m_t^{\overline{\text{MS}}}(m_t) = 168$ GeV and $m_b = 4.8$ GeV. Further $\alpha_s(M_Z) = 0.118$ [29], which corresponds to $\alpha_s(4.8\text{GeV}) = 0.216$. In the table $C_8^{(0)} = C_8^{(0),eff}$ is the scheme independent coefficient mentioned in the appendix.

In the LO the decays $b \rightarrow s\bar{s}s$, $b \rightarrow s\bar{s}d$, $b \rightarrow d\bar{d}s$ and $b \rightarrow d\bar{d}d$ can only proceed via Q_{3-6} and Q_8 , while $b \rightarrow u\bar{u}d$ and $b \rightarrow u\bar{u}s$ also receive contributions from Q_1 and Q_2 . We combine both cases in

$$\begin{aligned} \Gamma^{(0)} = & \frac{G_F^2 m_b^5}{64\pi^3} \left[t \sum_{i,j=1}^2 |\xi_u|^2 C_i^{(0)} C_j^{(0)} b_{ij} + \sum_{i,j=3}^6 |\xi_t|^2 C_i^{(0)} C_j^{(0)} b_{ij} \right. \\ & \left. - 2t \sum_{\substack{i=1,2 \\ j=3,\dots,6}} C_i^{(0)} C_j^{(0)} \text{Re}(\xi_u^* \xi_t) b_{ij} \right] \end{aligned} \quad (18)$$

with $t = 1$ for $q = u$ and $t = 0$ for $q = d, s$. The b_{ij} 's read

$$b_{ij} = \frac{16\pi^3}{m_b^6} \int \frac{d^3 \vec{p}_q d^3 \vec{p}_{\bar{q}} d^3 \vec{p}_d}{(2\pi)^5 8 |E_q E_{\bar{q}} E_d|} \delta^{(4)}(p_b + p_{\bar{q}} - p_q - p_d) \overline{\langle Q_i \rangle^{(0)} \langle Q_j \rangle^{(0)*}} = b_{ji} \quad (19)$$

with $Q_{1,2} = Q_{1,2}^u$ here. Setting the final state quark masses to zero one finds

$$b_{ij} = \begin{cases} 1 + r/3 & \text{for } i, j \leq 4, \text{ and } i + j \text{ even} \\ 1/3 + r & \text{for } i, j \leq 4, \text{ and } i + j \text{ odd} \end{cases}, \quad \begin{aligned} b_{55} &= b_{66} = 1, \\ b_{56} &= b_{65} = 1/3. \end{aligned} \quad (20)$$

Here $r = 1$ for the decays $b \rightarrow d\bar{d}d$ and $b \rightarrow s\bar{s}s$, in which the final state contains two identical particles, and $r = 0$ otherwise. The remaining b_{ij} 's are zero. Clearly for the $q \neq u$ the b_{ij} 's as defined in (19) vanish, if $i \leq 2$ or $j \leq 2$. Yet in the formulae for the decay rate we prefer to stress



Figure 4: The two diagrams contributing to $\Gamma^{(0)}$ in (18). The crosses represent any of Q_{1-6} .

this fact by keeping the parameter t , which switches the current-current effects off in the penguin induced decays. Our results in (20) agree with the zero mass limit of [9, 10]. The b_{ij} 's of (19) are visualized in Fig. 4.

$\Delta\Gamma_W$ simply reads

$$\begin{aligned} \Delta\Gamma_W = & \frac{G_F^2 m_b^5}{64\pi^3} 2 \left[t \sum_{i,j=1}^2 |\xi_u|^2 [C_i^{(0)} \Delta C_j] b_{ij} + \sum_{i,j=3}^6 |\xi_t|^2 [C_i^{(0)} \Delta C_j] b_{ij} \right. \\ & \left. - t \sum_{\substack{i=1,2 \\ j=3,\dots,6}} [C_i^{(0)} \Delta C_j + \Delta C_i C_j^{(0)}] \operatorname{Re} (\xi_u^* \xi_t) b_{ij} \right]. \end{aligned} \quad (21)$$

The current-current type corrections proportional to $C_{1,2}^{(0)} \cdot C_{1,2}^{(0)}$ are [8, 20, 23]

$$\Delta\Gamma_{cc} = t \frac{G_F^2 m_b^5}{64\pi^3} 2 |\xi_u|^2 \sum_{i,j=1}^2 C_i^{(0)} C_j^{(0)} h_{ij} \quad (22)$$

with t defined after (18). In the NDR scheme with the standard definition of the evanescent operators [30] the diagrams of Fig. 1, the bremsstrahlung diagrams and the subsequent phase space integrations yield [8]:

$$h_{11}^{NDR} = h_{22}^{NDR} = \frac{31}{3} - \frac{4}{3}\pi^2, \quad h_{12}^{NDR} \left(\frac{\mu}{m_b} \right) = h_{21}^{NDR} \left(\frac{\mu}{m_b} \right) = \frac{8}{3} \ln \frac{m_b^2}{\mu^2} - \frac{17}{3} - \frac{4}{9}\pi^2. \quad (23)$$

The inclusion of $\Delta\Gamma_{cc}$ is necessary to fix the definition of the b-quark mass entering $\Gamma^{(0)}$ in (18). The values quoted in (23) correspond to the use of the (one-loop) pole quark mass in (18).

In the same way we write

$$\begin{aligned} \Delta\Gamma_{peng} = & \frac{G_F^2 m_b^5}{64\pi^3} 2 \operatorname{Re} \left[t \sum_{i,j=1,2} C_i^{(0)} C_j^{(0)} \xi_u [\xi_c^* g_{ij}(x_c) + \xi_u^* g_{ij}(0)] \right. \\ & \left. - \sum_{\substack{i=1,2 \\ j=3,\dots,6}} C_i^{(0)} C_j^{(0)} \xi_t [\xi_c^* g_{ij}(x_c) + \xi_u^* g_{ij}(0)] \right]. \end{aligned} \quad (24)$$

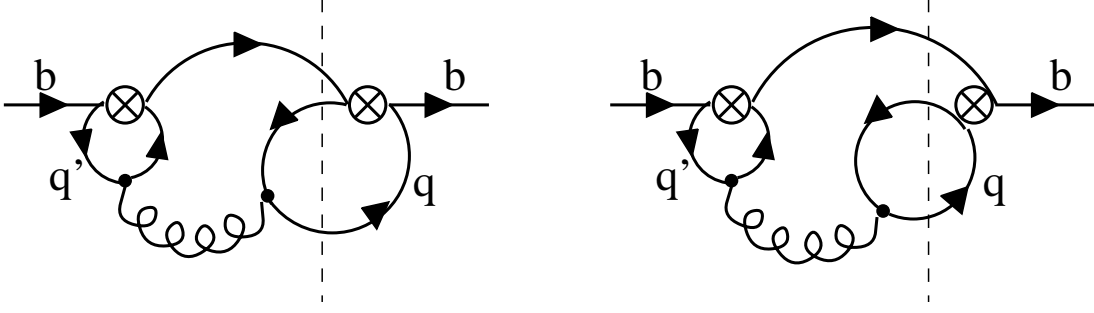


Figure 5: The diagrams contributing to $\Delta\Gamma_{peng}$ in (24). The left cross denotes $Q_1^{q'}$ or $Q_2^{q'}$ with $q' = u, c$ and the right cross represents any of Q_{1-6} . The dashed line indicates the final state with q being u, d or s .

Here g_{ij} is visualized in Fig. 5 and defined by

$$g_{ij} \left(x_{q'}, \frac{\mu}{m_b} \right) = \frac{16\pi^3}{m_b^6} \int \frac{d^3 \vec{p}_q d^3 \vec{p}_{\bar{q}} d^3 \vec{p}_d}{(2\pi)^5 8 |E_q E_{\bar{q}} E_d|} \delta^{(4)}(p_b + p_{\bar{q}} - p_q - p_d) \cdot \overline{\langle Q_i^{q'} \rangle_{peng}^{(1)} \langle Q_j \rangle^{(0)*}} \quad (25)$$

with $x_{q'} = m_{q'}/m_b$. We do not display the μ -dependence of the C_j 's, h_{ij} 's and g_{ij} 's in formulae for the decay rate such as (22) or (24) to simplify the notation. Now $\Delta\Gamma_{peng}$ in (24) is more complicated than $\Delta\Gamma_{cc}$ in (22) for two reasons: First interference terms of different CKM structures appear and second the internal quark in the penguin graph of Fig. 2 can be $q' = c$ or $q' = u$. Further the charm quark mass enters g_{ij} with $x_c = m_c/m_b$.

Finally $\Delta\Gamma_8$ in (16) is given by

$$\Delta\Gamma_8 = \frac{G_F^2 m_b^5}{64\pi^3} 2 \operatorname{Re} \left[-t \xi_u^* \xi_t C_8^{(0)} \sum_{j=1}^2 C_j^{(0)} b_{j8} + |\xi_t|^2 C_8^{(0)} \sum_{j=3}^6 C_j^{(0)} b_{j8} \right]. \quad (26)$$

Here the tree-level diagrams with Q_8 already contribute to order α_s .

The phase space integrations are contained in the coefficients b_{j8} in (26). They are depicted in Fig. 6 and are defined as

$$b_{j8} = \frac{16\pi^3 4\pi}{m_b^6 \alpha_s} \int \frac{d^3 \vec{p}_q d^3 \vec{p}_{\bar{q}} d^3 \vec{p}_d}{(2\pi)^5 8 |E_q E_{\bar{q}} E_d|} \delta^{(4)}(p_b + p_{\bar{q}} - p_q - p_d) \overline{\langle Q_j \rangle^{(0)} \langle Q_8 \rangle^{(0)*}} = b_{8j}. \quad (27)$$

It is instructive to insert the above expressions for $\Delta\Gamma_{cc}$, $\Delta\Gamma_{peng}$ and $\Delta\Gamma_8$ into (16). The decay rate then reads

$$\Gamma = \frac{G_F^2 m_b^5}{64\pi^3} \operatorname{Re} \left\{ t \sum_{i,j=1}^2 C_i C_j \left[|\xi_u|^2 b_{ij} + \frac{\alpha_s(\mu)}{4\pi} |\xi_u|^2 2 [h_{ij} + g_{ij}(0) - g_{ij}(x_c)] - \frac{\alpha_s(\mu)}{4\pi} \xi_u \xi_t^* 2 g_{ij}(x_c) \right] \right\}$$

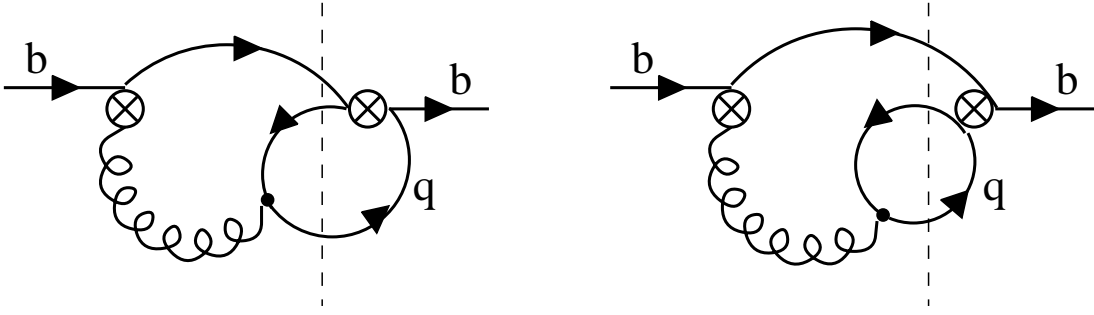


Figure 6: The diagrams contributing to $\Delta\Gamma_8$ in (26). The left cross denotes Q_8 and the right cross represents any of Q_{1-6} .

$$\begin{aligned}
 & - 2 \sum_{\substack{i=1,2 \\ j=3,\dots,6}} C_i C_j \left[t \xi_u^* \xi_t b_{ij} + \frac{\alpha_s(\mu)}{4\pi} \xi_u^* \xi_t [g_{ij}(0) - g_{ij}(x_c)] - \frac{\alpha_s(\mu)}{4\pi} |\xi_t|^2 g_{ij}(x_c) \right] \\
 & + \sum_{i,j=3}^6 C_i C_j |\xi_t|^2 b_{ij} \\
 & + \frac{\alpha_s(\mu)}{4\pi} C_8 \left[-t \xi_u^* \xi_t \sum_{j=1}^2 C_j 2 b_{j8} + |\xi_t|^2 \sum_{j=3}^6 C_j 2 b_{j8} \right] \}.
 \end{aligned} \tag{28}$$

Here the C_j 's are the Wilson coefficients of (17) including NLO corrections. $C_j^{(0)}$ rather than C_j^{NDR} should be used in the terms of order α_s in (28) for consistency. The unitarity of the CKM matrix has been used to eliminate ξ_c from (28).

From (24) or (28) one notices that penguin induced decays with $t = 0$ receive radiative corrections proportional to the large coefficient C_2 , which does not enter the tree-level decay rate in (18). Further $\Delta\Gamma_{peng}$ depends on the CKM phase δ , because ξ_u , ξ_t and the loop functions g_{ij} are complex. Decay rates and CP asymmetries for these penguin induced decays have been derived in [19] in terms of a two-fold integral representation taking into account the interference of the penguin diagram involving Q_2 with Q_{1-6} . In sect. 3 we derive analytical results for the decay rates and also include $\Delta\Gamma_8$.

In the decays $b \rightarrow u\bar{u}d$ and $b \rightarrow u\bar{u}s$ the main focus is on the first sum in $\Delta\Gamma_{peng}$ in (24) containing products of two of the large coefficients C_1 and C_2 . We also keep the second sum in (24), but remark here that these terms are not the full set of one-loop radiative corrections involving one large coefficient $C_{1,2}$ and one small coefficient C_{3-6} : In addition to the radiative corrections calculated in this paper there are also current-current diagrams (see Fig. 1) and penguin diagrams (see Fig. 2) with penguin operators Q_{3-6} . In decays with a (u, \bar{u}) -pair in the final state these matrix elements interfere with those of Q_1^u and Q_2^u and therefore also yield a term proportional to $C_{1,2} \cdot C_{3-6}$.

The terms proportional to $C_j \cdot C_8$ comprised in $\Delta\Gamma_8$ are interesting in order to confirm or falsify the mechanism proposed in [17]. If new physics indeed dominates C_8 , then $\Gamma(b \rightarrow s + g) \propto |C_8|^2$ considered in [17] is enhanced. Yet $\Delta\Gamma_8$ is linear in C_8 , so that the sign of the new physics

contribution may determine whether $\Gamma(b \rightarrow \text{no charm})$ is enhanced or diminished. A calculation similar to ours has been partly done in [31]. Yet in [31] some questionable approximations have been made: For example the operator mixing has been neglected and the top quark has not been integrated out but instead formally treated as a light particle. In some cases the results of [31] differ substantially from those in [19].

We close this section with the formula relating Γ in (28) to the $r_{q_1 \bar{q}_2 q_3}$'s defined in (6). To this end we need the semileptonic decay rate to order α_s [32]:

$$\Gamma(b \rightarrow c e \bar{\nu}_e) = \frac{G_F^2 m_b^5}{192\pi^3} |V_{cb}|^2 f_1(x_c^2) \left[1 + \frac{\alpha_s(\mu)}{2\pi} h_{SL}(x_c) + O(\alpha_s^2) \right].$$

The tree-level phase space function is

$$f_1(a) = 1 - 8a - 12a^2 \ln a + 8a^3 - a^4.$$

The analytic expression for $h_{SL}(x_c)$ can be found in [8, 32]. The approximation

$$h_{SL}(x_c) = -3.341 + 4.05(x_c - 0.3) - 4.3(x_c - 0.3)^2$$

holds to an accuracy of 1 permille in the range $0.2 \leq x_c \leq 0.4$. Here $x_c = m_c/m_b$ is the ratio of the one-loop pole masses. We further include the hadronic corrections to the free quark decay of order $1/m_b^2$ obtained from the HQE [3]. This yields

$$r_{q\bar{q}d} = \frac{192\pi^3}{G_F^2 m_b^5 |V_{cb}|^2 f_1(x_c^2)} \left\{ \Gamma + \Gamma^{(0)} \left[6 \left(\frac{(1-x_c^2)^4}{f_1(x_c^2)} - 1 \right) \frac{\lambda_2}{m_b^2} - \frac{\alpha_s(\mu)}{2\pi} h_{SL}(x_c) \right] + \delta\Gamma \right\}. \quad (29)$$

Here $\lambda_2 = 0.12 \text{ GeV}^2$ encodes the chromomagnetic interaction of the b-quark with the light degrees of freedom. Further corrections are contained in $\delta\Gamma$. It is obtained from $\Gamma^{(0)}$ by substituting b_{ij} with δb_{ij} in the definition (18). One finds from [3]:

$$\delta b_{12} = \delta b_{14} = \delta b_{21} = \delta b_{23} = \delta b_{32} = \delta b_{34} = \delta b_{41} = \delta b_{43} = -8 \frac{\lambda_2}{m_b^2} = -0.042 \quad \text{for } m_b = 4.8 \text{ GeV},$$

while $\delta b_{56} = \delta b_{65}$ is unknown yet. If there are no identical quarks in the final state, the remaining δb_{ij} 's vanish. Otherwise

$$\delta b_{33} = \delta b_{44} = \delta b_{34}, \quad \delta b_{55} = \delta b_{66} \neq 0 \quad \text{for } b \rightarrow d\bar{d} \text{ and } b \rightarrow s\bar{s} \quad (30)$$

with δb_{66} unknown. The dependence on λ_1 parameterizing the effect of the b-quark's Fermi motion on the decay rates cancels in the ratio in (29).

For the calculation of r_ℓ in (7) we also need r_{ue} and r_{sg} . The corresponding expressions are [3, 27]:

$$\begin{aligned} r_{ue} &= \left| \frac{V_{ub}}{V_{cb}} \right|^2 \frac{1}{f_1(x_c^2)} \left[1 + \frac{\alpha_s(\mu)}{2\pi} [h_{SL}(0) - h_{SL}(x_c)] + 6 \left[\frac{(1-x_c^2)^4}{f_1(x_c^2)} - 1 \right] \frac{\lambda_2}{m_b^2} \right], \\ r_{sg} &= \left| \frac{V_{tb}^* V_{ts}}{V_{cb}} \right|^2 \frac{8 \alpha_s(\mu)}{\pi f_1(x_c^2)} [C_8(\mu)]^2. \end{aligned}$$

3. Calculation

This section is devoted to the calculation of the g_{ij} 's and b_{j8} 's entering (24,26,28). All results correspond to the NDR scheme.

The first step is the same for all b-decays under consideration: The penguin diagram of Fig. 2 must be calculated to obtain the r_{ij} 's in (15):

$$\begin{aligned} r_{24}(p^2, m, \mu) &= \frac{1}{3} \log \frac{m^2}{\mu^2} - \frac{2}{9} - \frac{4m^2}{3p^2} \\ &\quad - \frac{1}{3} \left(1 + \frac{2m^2}{p^2}\right) \sqrt{1 - \frac{4m^2}{p^2} + i\delta} \log \frac{\sqrt{1 - \frac{4m^2}{p^2} + i\delta} - 1}{\sqrt{1 - \frac{4m^2}{p^2} + i\delta} + 1}, \\ r_{24}(p^2, 0, \mu) &= \frac{1}{3} \left[\log \frac{p^2}{\mu^2} - i\pi \right] - \frac{2}{9}, \end{aligned} \quad (31)$$

$$r_{26} = r_{24}, \quad r_{23} = r_{25} = -\frac{1}{3}r_{24}. \quad (32)$$

Here $p = p_b - p_d$ is the momentum flowing through the gluon leg and m is the internal quark mass. The infinitesimal “ $i\delta$ ”-prescription yields the correct sign of the imaginary part of the logarithm in the case $p^2 > 4m^2$ and likewise regulates the square root for $p^2 < 4m^2$. The r_{1j} 's and r_{28} are zero.

Next we combine (25) and (15) to obtain the coefficients g_{ij} in (24) and (28):

$$\begin{aligned} g_{ij} \left(x_c, \frac{\mu}{m_b} \right) &= \frac{16\pi^3}{m_b^6} \int \frac{d^3 \vec{p}_q d^3 \vec{p}_{\bar{q}} d^3 \vec{p}_d}{(2\pi)^5 8 |E_q E_{\bar{q}} E_d|} \delta^{(4)}(p_b + p_{\bar{q}} - p_q - p_d) \cdot \\ &\quad \sum_{k=1}^6 r_{ik}^c \left((p_b - p_d)^2, x_c m_b, \mu \right) \overline{\langle Q_k \rangle^{(0)} \langle Q_j \rangle^{(0)*}}. \end{aligned} \quad (33)$$

The corresponding expression for an internal u -quark is obtained by substituting c with u in (33). For the decays $b \rightarrow u\bar{u}d$, $b \rightarrow u\bar{u}s$, $b \rightarrow s\bar{s}d$ and $b \rightarrow d\bar{d}s$ one finds:

$$\begin{aligned} g_{22} \left(x_c, \frac{\mu}{m_b} \right) &= g_{24} \left(x_c, \frac{\mu}{m_b} \right) = g_{26} \left(x_c, \frac{\mu}{m_b} \right) = \\ &\quad \frac{16}{27} \ln \frac{x_c m_b}{\mu} - \frac{16}{27} \left(1 - 10x_c^2 + 18x_c^4 - 36x_c^6 \right) \sqrt{1 - 4x_c^2} \ln \frac{1 - \sqrt{1 - 4x_c^2}}{2x_c} \\ &\quad + \frac{4}{9} \left[-\frac{3}{2} + 16x_c^2 - 14x_c^4 + 24x_c^6 + 32x_c^6 (2 - 3x_c^2) \left(\ln^2 \frac{1 - \sqrt{1 - 4x_c^2}}{2x_c} - \frac{\pi^2}{4} \right) \right] \\ &\quad - i\pi \frac{4}{9} \left[\frac{2}{3} \sqrt{1 - 4x_c^2} \left(1 - 10x_c^2 + 18x_c^4 - 36x_c^6 \right) - 32x_c^6 (2 - 3x_c^2) \ln \frac{1 - \sqrt{1 - 4x_c^2}}{2x_c} \right] \end{aligned}$$

$$\begin{aligned}
g_{22} \left(0, \frac{\mu}{m_b} \right) &= g_{24} \left(0, \frac{\mu}{m_b} \right) = g_{26} \left(0, \frac{\mu}{m_b} \right) = \frac{4}{9} \left[-\frac{3}{2} + \frac{4}{3} \ln \frac{m_b}{\mu} - \frac{2}{3} i\pi \right] \\
g_{21} \left(x, \frac{\mu}{m_b} \right) &= g_{23} \left(x, \frac{\mu}{m_b} \right) = g_{25} \left(x, \frac{\mu}{m_b} \right) = g_{1j} \left(x, \frac{\mu}{m_b} \right) = 0, \quad j = 1, \dots, 6,
\end{aligned} \tag{34}$$

where $x_c = m_c/m_b$. Numerically one finds for actual quark masses:

$$g_{22} (0, 1) = -0.67 - 0.93 i, \quad g_{22} (0.3, 1) = -0.69 - 0.23 i. \tag{35}$$

The near equality of the real parts in (35) is a numerical accident.

In the case of two identical particles in the final state both diagrams of Fig. 5 contribute. Then g_{23} is no more zero, but

$$g_{23} \left(x, \frac{\mu}{m_b} \right) = g_{22} \left(x, \frac{\mu}{m_b} \right) \quad \text{for } b \rightarrow d\bar{d}d \text{ and } b \rightarrow s\bar{s}s. \tag{36}$$

The remaining g_{ij} 's are as in (34). As an analytical check we have confirmed that the μ -dependence in (34) and (36) cancels with the μ -dependence in the Wilson coefficients in (18) to order α_s .

We now turn to the calculation of $\Delta\Gamma_8$ in (26). Performing the phase space integration in (27) yields

$$\begin{aligned}
b_{28} &= b_{48} = b_{68} = -\frac{16}{9}, \\
b_{18} &= b_{38} = b_{58} = 0
\end{aligned} \tag{37}$$

for $b \rightarrow u\bar{u}d$, $b \rightarrow u\bar{u}s$, $b \rightarrow s\bar{s}d$ and $b \rightarrow d\bar{d}s$. If identical particles are present, b_{38} is no more zero, but instead reads

$$b_{38} = -\frac{16}{9} \quad \text{for } b \rightarrow d\bar{d}d \text{ and } b \rightarrow s\bar{s}s. \tag{38}$$

The remaining b_{j8} 's are as in (37).

4. Charmless decay rates

4.1. Standard Model

In this section we discuss our numerical results for the various decay rates. We use the following set of input parameters:

$$\begin{aligned}
\left| \frac{V_{ub}}{V_{cb}} \right| &= 0.08 \pm 0.02, & \delta &= 90^\circ \pm 30^\circ, & x_c &= 0.29 \pm 0.04, & \mu &= m_b = 4.8 \text{ GeV}, \\
\alpha_s (M_Z) &= 0.118, & |V_{cb}| &= 0.038, & m_t (m_t) &= 168 \text{ GeV}.
\end{aligned} \tag{39}$$

The $r_{q\bar{q}q'}$'s sizeably depend on $|V_{ub}/V_{cb}|$, δ , x_c and especially on the renormalization scale, which will be varied in the range $m_b/2 \leq \mu \leq 2m_b$. The quark masses in (39) are taken from [33], the

		final state							
		input	$u\bar{u}d$	$u\bar{u}s$	$d\bar{d}s$	$s\bar{s}s$	$s\bar{s}d$	$d\bar{d}d$	no charm
$r_{q\bar{q}q'}$	as in (39)	0.040	0.021	0.018	0.015	$8.9 \cdot 10^{-4}$	$7.2 \cdot 10^{-4}$	0.14	
	$\mu = m_b/2$	0.044	0.033	0.029	0.024	$14.0 \cdot 10^{-4}$	$11.4 \cdot 10^{-4}$	0.19	
	$\mu = 2m_b$	0.037	0.014	0.011	0.009	$5.5 \cdot 10^{-4}$	$4.6 \cdot 10^{-4}$	0.11	
	$ V_{ub}/V_{cb} = 0.06$	0.023	0.020	0.018	0.015	$8.7 \cdot 10^{-4}$	$7.1 \cdot 10^{-4}$	0.11	
	$ V_{ub}/V_{cb} = 0.10$	0.062	0.023	0.018	0.015	$9.1 \cdot 10^{-4}$	$7.5 \cdot 10^{-4}$	0.18	
	$\delta = 60^\circ$	0.044	0.017	0.018	0.015	$5.9 \cdot 10^{-4}$	$4.8 \cdot 10^{-4}$	0.14	
	$\delta = 120^\circ$	0.036	0.025	0.018	0.014	$12.2 \cdot 10^{-4}$	$10.0 \cdot 10^{-4}$	0.14	
	$x_c = 0.25$	0.034	0.019	0.016	0.013	$8.1 \cdot 10^{-4}$	$6.7 \cdot 10^{-4}$	0.12	
	$x_c = 0.33$	0.048	0.023	0.020	0.017	$9.7 \cdot 10^{-4}$	$7.9 \cdot 10^{-4}$	0.16	
Br	as in (39)	0.41%	0.22%	0.18%	0.15%	$9.1 \cdot 10^{-3}\%$	$7.4 \cdot 10^{-3}\%$	1.4%	

Table 2: The values of $r_{q\bar{q}q'}$ for the various final states as defined in (6). The input parameters are chosen as in (39) except for the quantity listed in the second column. The last column lists r_ϕ defined in (7). Br in the last row is the branching ratio for $B \rightarrow X_{q\bar{q}q'}$ obtained by multiplying $r_{q\bar{q}q'}$ with $B_{SL} = 10.23\%$.

values for $|V_{ub}/V_{cb}|$ and $|V_{cb}|$ have been presented in [34]. The range for the CKM phase δ has been obtained from the NLO analysis of ϵ_K and Δm_B in [35]. The dependence on $\alpha_s(M_Z)$ in the range $0.112 \leq \alpha_s(M_Z) \leq 0.124$ [29] is weaker than the μ -dependence. Our results are listed in Tab. 2.

Keeping the physical input parameters as in (39) and varying the scale in the range $m_b/2 \leq \mu \leq 2m_b$ the charmless decay modes sum to

$$r_\phi = 0.15 \pm 0.04.$$

The values for r_{sg} and r_{ue} entering this result are

$$r_{sg} = 0.02 \pm 0.01, \quad r_{ue} = 0.01 \pm 0.00.$$

Incorporating also the uncertainties in $|V_{ub}/V_{cb}|$ and x_c one finds

$$r_\phi = 0.15 \pm 0.08. \quad (40)$$

final state	$\propto C_{1,2}^{(0)} \cdot C_{1,2}^{(0)}$	$\propto C_{3-6}^{(0)} \cdot C_{1-6}^{(0)}$	$\propto \Delta\bar{\Gamma}_W$	$\propto \Delta\bar{\Gamma}_{cc}$	$\propto \Delta\bar{\Gamma}_{peng}$	$\propto \Delta\bar{\Gamma}_8$
$u\bar{u}d$	107	-4	-5	6	-5	1
$u\bar{u}s$	10	39	-7	1	72	-14
$d\bar{d}s$	0	46	-8	0	78	-16
$s\bar{s}s$	0	44	-20	0	92	-16
$s\bar{s}d$	0	54	-9	0	74	-19
$d\bar{d}d$	0	52	-24	0	91	-19
sg	0	0	0	0	0	100
no charm	46	17	-6	2	31	11

Table 3: Separate contributions to $\Gamma(b \rightarrow q\bar{q}q')$ in percent of the total rate for the input parameters of (39). In the third column the contribution from the LO matrix elements of penguin operators and their interference with matrix elements of $Q_{1,2}$ is shown. In the last row $\Gamma(b \rightarrow ue\bar{\nu}_e)$ entering r_ϕ has been assigned to the second column listing the current-current part.

To discuss the results for the individual charmless decay modes it is instructive to look at the separate scheme-independent contributions from $\Gamma^{(0)}$, $\Delta\bar{\Gamma}_{cc}$, $\Delta\bar{\Gamma}_{peng}$, $\Delta\bar{\Gamma}_8$ and $\Delta\bar{\Gamma}_W$ (cf. the appendix) to the decay rate. These contributions are listed in Tab. 3, in which also the contributions from penguin operators to $\Gamma^{(0)}$ are shown.

All decays except for $B \rightarrow X_{u\bar{u}d}$ are dominated by penguin effects. The sizeable μ -dependence in these decays can be reduced by calculating the current-current type radiative corrections to penguin operators. Note that all these decay rates are even dominated by the *penguin diagrams* calculated in this work. On the other hand the terms stemming from Q_8 lower the penguin induced rates. In $B \rightarrow no\ charm$, however, the net effect of Q_8 is positive because of the two-body decay $b \rightarrow sg$ proportional to C_8^2 .

The calculation of r_ϕ in [11] has included $\Gamma^{(0)}$, $\Delta\bar{\Gamma}_W$, and $\Delta\bar{\Gamma}_{cc}$. Taking into account that in [11] a high (theoretical) value for B_{SL} has been used, the result of [11] translates into

$$r_\phi = 0.14 \quad \text{for } \left| \frac{V_{ub}}{V_{cb}} \right| = 0.10.$$

The corresponding value in Tab. 2 is $r_\phi = 0.18$ showing the increase due to $\Delta\bar{\Gamma}_{peng} + \Delta\bar{\Gamma}_8$.

Despite of the 36 % increase in r_ϕ in (40) the value is still much below $r_\phi = 1.0 \pm 0.4$ needed to solve the missing charm puzzle. The new theoretical prediction for n_c is

$$n_c = 1.33 \mp 0.06,$$

which is only marginally lower than the old result in (4). Still an enhancement of r_ϕ by a factor between 2.6 and 20 is required. Yet with the result in (34) for the penguin diagram of Fig. 5 at hand we can estimate the non-perturbative enhancement of the (c, \bar{c}) intermediate state necessary to reproduce the experimental result. The mechanism proposed in [14, 18] corresponds to a violation of quark-hadron duality, which we may parametrize by multiplying the (c, \bar{c}) -penguin function $g_{ij}(x_c, \mu/m_b)$ in (28) by an arbitrary factor d . We find that d must be chosen as large as 20 in order to reach the lowest desired value $r_\phi = 0.6$ for the central set of the input parameters in (39). Yet in this case one must also include the double-penguin diagram obtained by squaring the result of Fig. 2. Taking this into account non-perturbative effects must still increase the (c, \bar{c}) -penguin diagram by roughly a factor of 9 over its short distance result in the NDR scheme. Having in mind that the phase space integration contained in $g_{ij}(x_c, \mu/m_b)$ implies a smearing of the invariant hadronic mass of the (c, \bar{c}) -pair such a large deviation of quark-hadron duality seems unlikely.

Our results for the branching fractions of $b \rightarrow d\bar{d}s$ and $b \rightarrow s\bar{s}s$ differ by roughly a factor of 1/2 from the results in [19]. The main source of the discrepancy is the different calculation of the total rate Γ_{tot} entering the theoretical definition of the branching fraction. Our predictions for the branching ratios in Tab. 2 contain the total rate via $\Gamma_{tot} = \Gamma_{SL}/B_{SL}^{exp}$, while in [19] $\Gamma_{tot} = G_F^2 m_b^5 |V_{cb}|^2 / (64\pi^3)$ has been used. This approximation neglecting the RG effects appears to be too crude and is responsible for 50 % of the discrepancy. The remaining difference is due to the effect of $\Delta\Gamma_8$ not considered in [19] and the use of different values of the Wilson coefficients. Our predictions for $Br(b \rightarrow s\bar{s}d)$ and $Br(b \rightarrow d\bar{d}d)$ are even smaller by a factor of 5 than the results of [19]. This is due to the fact that in addition the value of $|V_{td}/V_{cb}|^2$ used in [19] is more than twice as large as the present day value used in our analysis. We remark that with our new results the number of B-mesons to be produced in order to detect the inclusive CP asymmetries corresponding to these decays is substantially larger than estimated in [19].

4.2. New physics

In the Standard Model the initial conditions for C_{3-6} and C_8 are generated at a scale $\mu = O(M_W)$ by the one-loop bsg -vertex function with a W -boson and a top quark as internal particles. Due to the helicity structure of the couplings positive powers of m_t are absent in the bsg -vertex. In many extensions of the Standard model such a helicity suppression does not occur [17]. Further in supersymmetric extensions flavour changing transitions can be mediated by gluinos, whose coupling to (s)quarks involves the strong rather the weak coupling constant. Recently a possible enhancement of C_8 affecting r_{sg} and thereby r_ϕ has attracted much attention [17]. In the following we will perform a model independent analysis of this hypothesis.

New physics affects the initial condition of the Wilson coefficients calculated at the scale of the masses mediating the flavour-changing transition of interest. We will take $\mu = M_W$ as the initial scale for both the standard and non-standard contributions to the Wilson coefficients. The renormalization group evolution down to $\mu = m_b$ mixes the various initial values and can damp or enhance the new physics effects in $C_i(M_W)$. For example the Standard Model value of $C_8(4.8 \text{ GeV})$

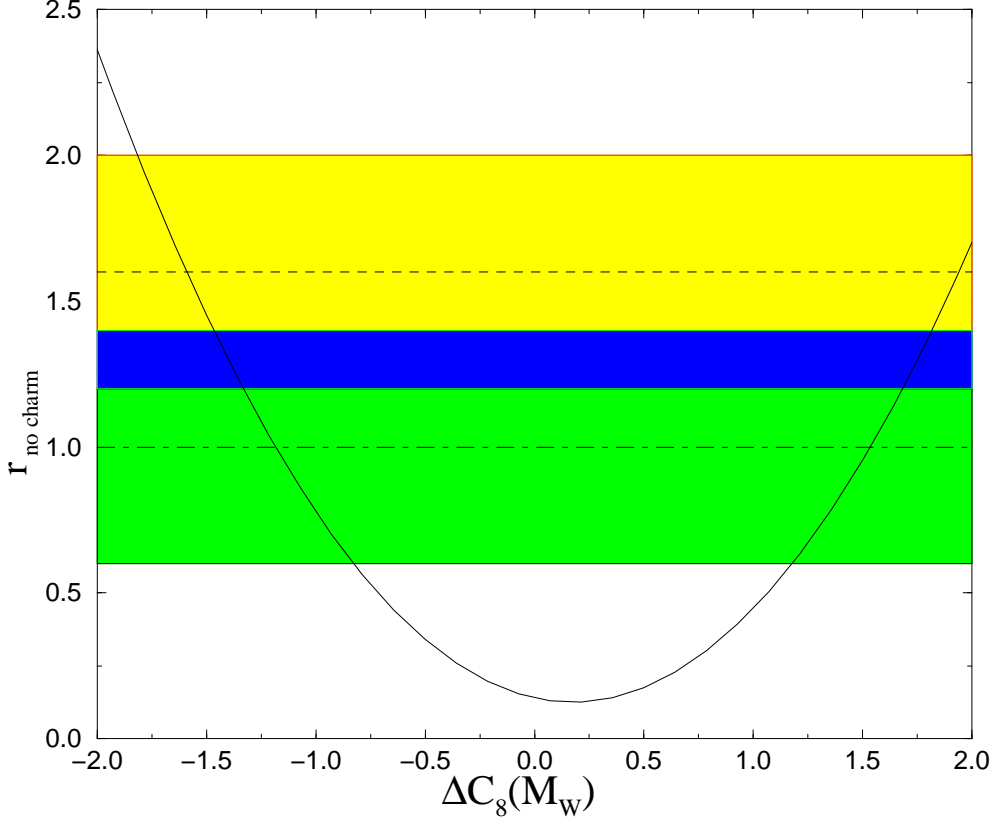


Figure 7: r_ϕ vs. $\Delta C_8(M_W)$ parameterizing new physics contributions to $C_8(M_W)$. The dark shading marks the region $r_\phi = 1.0 \pm 0.4$ needed to reproduce the experimental result for n_c in (1). The lightly shaded area corresponds to $r_\phi = 1.6 \pm 0.4$ obtained from the analysis in [14].

in Tab. 1 is mainly a linear combination of $C_2(M_W)$ and $C_8(M_W)$:

$$C_8(m_b) = -0.08 C_2(M_W) + 0.7 C_8(M_W)$$

with $C_8(M_W) = -0.1$. If one enlarges $C_8(M_W)$ by a factor of 10 while keeping $C_{1-6}(M_W)$ fixed, r_ϕ grows by a factor of 5.5. The sensitivity of r_ϕ to $C_{3-6}(M_W)$ is much smaller, increasing the latter by a factor of 10 enhances r_ϕ only by a factor of 1.6. Hence in the following we will only focus on $C_8(M_W) = -0.1 + \Delta C_8(M_W)$, where $\Delta C_8(M_W)$ is the new physics contribution. For simplicity we will further assume that the CKM structure of the new contributions is the same as in the Standard model and neglect the possibility of new CP-violating phases by assuming $\Delta C_8(M_W)$ to be real.

In Fig. 7 r_ϕ is plotted versus $\Delta C_8(M_W)$. Solving for $r_\phi = 1.0 \pm 0.4$ yields two solutions:

$$\Delta C_8(M_W) = -1.2 {}^{+0.3}_{-0.4}, \quad \Delta C_8(M_W) = 1.5 \pm 0.3. \quad (41)$$

The central values correspond to an enhancement of the Standard Model value for $C_8(M_W)$ by factors of 13 and (-14) . We hope to resolve the twofold ambiguity after calculating the contribution of Q_8 to $\Gamma(\bar{B} \rightarrow X_{c\bar{c}s})$.

The LEP data in (5) correspond to $r_d = 0.4 \pm 0.5$ and

$$\Delta C_8(M_W) = -0.5 \begin{array}{l} -0.6 \\ +0.5 \end{array}, \quad \Delta C_8(M_W) = 0.9 \begin{array}{l} +0.6 \\ -0.9 \end{array}$$

showing the consistency of (5) with the Standard Model.

5. Conclusions

We have calculated two new contributions to the inclusive decay rates of B-mesons into various charmless final states: First we have obtained the results of penguin diagrams involving the operator Q_2 and a c - or u -quark in the loop putting special care on the renormalization scheme independence of our results. Second we have calculated the influence of the chromomagnetic dipole operator Q_8 on these decays. The former contributions have been found to dominate the branching fractions for $\bar{B} \rightarrow X_{u\bar{u}s}$, $\bar{B} \rightarrow X_{d\bar{d}s}$, $\bar{B} \rightarrow X_{s\bar{s}s}$, $\bar{B} \rightarrow X_{s\bar{s}d}$ and $\bar{B} \rightarrow X_{d\bar{d}d}$. The effect of Q_8 on these decay modes is also sizeable and decreases the rates. On the other hand the decay rate for $\bar{B} \rightarrow X_{u\bar{u}d}$ is only affected by a few percent. Our results increase the theoretical prediction for $Br(B \rightarrow \text{no charm})$ by 36 %, which is not sufficient to explain the charm deficit observed in B-decays by ARGUS and CLEO. If a breakdown of quark-hadron duality due to intermediate (c, \bar{c}) resonances is to explain the “missing charm puzzle”, the phase space integrated penguin diagram with an internal c -quark must be larger than the perturbative result in the NDR scheme by roughly a factor of 9.

We have then analyzed the hypothesis that new physics effects enhance the coefficient C_8 of Q_8 and have performed a model independent fit of C_8 to the experimental data on n_c . The renormalization group evolution from $\mu = M_W$ to $\mu = m_b$ has been properly taken into account. One finds two solutions for C_8 : For the central values of the theoretical input and the data of the $\Upsilon(4S)$ experiments $C_8(M_W)$ must be larger by a factor of 13 or (-14) than in the Standard Model, if the new physics contributions have the same CKM structure as the Standard Model penguin diagram.

Acknowledgements

We are grateful to Andrzej Buras for many stimulating discussions. We thank him and Christoph Greub for proofreading the manuscript. U.N. acknowledges interesting discussions with Stefano Bertolini, Antonio Masiero and Yong-Yeon Keum.

A. Scheme independence

Now we discuss the cancellation of scheme dependent terms between the NLO Wilson coefficients and the loop diagrams contained in $\Delta\Gamma_{cc}$ and $\Delta\Gamma_{peng}$. We define scheme independent

combinations $\Delta\bar{\Gamma}_{cc}$, $\Delta\bar{\Gamma}_{peng}$ and $\Delta\bar{\Gamma}_W$, which allow a meaningful discussion of the numerical sizes of these separate contributions to Γ as performed in sect. 4. Finally we comment on the scheme independence of $\Delta\Gamma_8$.

The NLO correction to the Wilson coefficients in (17) can be split into two parts:

$$\Delta C_j(\mu) = \sum_{k=1}^6 J_{jk} C_k^{(0)}(\mu) + \Delta\bar{C}_j(\mu), \quad j = 1, \dots, 6. \quad (42)$$

$\Delta\bar{C}_j(\mu)$ contains the contributions stemming from the weak scale. It is independent of the renormalization scheme and proportional to $\alpha_s(M_W)/\alpha_s(\mu)$. Yet the J_{jk} 's in (42) are scheme dependent. The precise definitions of the terms in (42) can be found in [28, 30]. We now absorb the terms involving J_{jk} into $\Delta\bar{\Gamma}_{cc}$ and $\Delta\bar{\Gamma}_{peng}$, so that the latter become scheme independent.

The identification of scheme independent combinations of one-loop matrix elements and J_{jk} 's is most easily done, if one expresses the loop diagrams in terms of the tree-level matrix elements. The combination

$$r_{jk}^{q'}(p^2, m_{q'}, \mu) + J_{kj}, \quad j \leq 2 \text{ and } k \geq 3, \quad (43)$$

of the coefficients in (15) and the J_{kj} 's is scheme independent [28]. Substituting $r_{jk}^{q'}$ with (43) in (33) one finds the scheme independent quantity:

$$\begin{aligned} \Delta\bar{\Gamma}_{peng} = & \Delta\Gamma_{peng} + \frac{G_F^2 m_b^5}{64\pi^3} 2 \operatorname{Re} \left[-t \xi_u \xi_t^* \sum_{\substack{i,j=1,2 \\ k=3,\dots,6}} C_i^{(0)} C_j^{(0)} J_{ki} b_{jk} \right. \\ & \left. + |\xi_t|^2 \sum_{\substack{i=1,2 \\ j,k=3,\dots,6}} C_i^{(0)} C_j^{(0)} J_{ki} b_{jk} \right]. \end{aligned} \quad (44)$$

Here $\xi_t^* = -\xi_u^* - \xi_c^*$ has been used. In the NDR scheme the J_{ki} 's in (44) evaluate to [28]

$$\begin{aligned} J_{31} &= -0.877, & J_{32}^{NDR} &= -0.532, \\ J_{41} &= 0.324, & J_{42}^{NDR} &= -0.202, \\ J_{51} &= 0.557, & J_{52}^{NDR} &= 0.511, \\ J_{61} &= 0.146, & J_{62}^{NDR} &= -0.677. \end{aligned} \quad (45)$$

The J_{k1} 's in the first row of (45) do not depend on the renormalization scheme, because $r_{1j}^{q'} = 0$ in all schemes due to a vanishing colour factor.

In the same way one finds

$$\Delta\bar{\Gamma}_{cc} = t \frac{G_F^2 m_b^5}{64\pi^3} 2 |\xi_u|^2 \sum_{i,j=1}^2 C_i^{(0)} C_j^{(0)} \left[h_{ij} + \sum_{k=1}^2 J_{ki} b_{kj} \right]. \quad (46)$$

Here the scheme dependence of the h_{ij} 's in (23) cancels with the one of the J_{ki} 's [28]:

$$J_{11}^{NDR} = J_{22}^{NDR} = \frac{631}{6348} = 0.099, \quad J_{12}^{NDR} = J_{21}^{NDR} = \frac{3233}{2116} = 1.528. \quad (47)$$

If one inserts (42) into $\Delta\Gamma_W$, one finds the J_{jk} 's with $k \leq 2$ to appear exactly in the combinations entering (44) and (46). The remaining J_{jk} 's with $k \geq 3$ describing penguin-penguin mixing would cancel the scheme dependence of the loop diagrams of Fig. 1 and Fig. 2 with insertions of penguin operators Q_j , $j = 3, \dots, 6$. Since the latter are omitted in our calculation, we must also leave out the J_{jk} 's with $k \geq 3$ in (42). This has been done in Tab. 1. $\Delta\bar{C}_j$ has been tabulated in the last line of Tab. 1 for illustration. It can be obtained from the other entries of the table with the help of (42), (47) and (45).

Finally $\Delta\bar{\Gamma}_W$ is simply obtained from $\Delta\Gamma_W$ in (21) by replacing ΔC_j with $\Delta\bar{C}_j$.

Unlike $C_j^{(0)}$, $j \leq 6$, $C_8^{(0)}$ is a two-loop quantity and therefore a priori scheme dependent. We understand H in (12) to be renormalized such that the matrix elements $\langle dg | Q_j | b \rangle$ vanish at the one-loop level for $j = 1, \dots, 6$. This ensures that $\Delta\Gamma_8$ as defined in (26) is scheme independent [27]. The thereby renormalized LO coefficient $C_8^{(0)}$ is usually called \tilde{C}_8 or $C_8^{(0),eff}$. In the NDR scheme this finite renormalization simply amounts to $C_8^{(0)} = C_8^{(0),NDR} + C_5^{(0)}$. Apart from $\Delta\Gamma_8$ this only affects the penguin diagram of Q_5 (cf. Fig. 2), which is a part of the neglected radiative corrections to penguin operators.

References

- [1] T.E. Browder, K. Honscheid and D. Pedrini, hep-ph/9606354, to appear in *Annual Review of Nuclear and Particle Science*.
T.E. Browder, hep-ph/9611373, talk at the *ICHEP conference* 1996, Warsaw, to appear in the proceedings.
J.D. Richman, hep-ex/9701014, talk at the *ICHEP conference*, Warsaw, 1996.
- [2] B. Barish *et al.* (CLEO), Phys. Rev. Lett. 76 (1996) 1570.
H. Albrecht *et al.* (ARGUS), Phys. Lett. B318 (1993) 397.
- [3] I.I. Bigi, N. Uraltsev, and A. Vainshtein, Phys. Lett. B 293, 430 (1992); Erratum *ibid.* 297, 477 (1993).
B. Blok and M. Shifman, Nucl. Phys. B399 (1993) 441; *ibid.* 399 (1993) 459.
- [4] A. Manohar and M. Wise, Phys. Rev. D 49, (1994) 1310.
B. Blok, L. Koprakh, M. Shifman and A.I. Vainshtein, Phys. Rev. D49 (1994), 3356; Erratum *ibid.* D50 (1994) 3572.
T. Mannel, Nucl. Phys. B413 (1994) 396.
I.I. Bigi, M.A. Shifman, N.G. Uraltsev, A.I. Vainshtein, Int. J. Mod. Phys. A9 (1994) 2467.
- [5] I.I. Bigi, B. Blok, M. Shifman, N. Uraltsev and A. Vainshtein, in *B decays*, ed. S. Stone, 2nd edition, *World Scientific*, Singapore, 1994, 132.
I.I. Bigi, hep-ph/9508408.

- [6] M. Neubert and C. Sachrajda, hep-ph/9603202.
- [7] I.J. Kroll, hep-ex/9602005, proceedings of the *17th Int. Symp. on Lepton Photon Interactions*, Beijing, P.R. China, 1995, 204.
- [8] E. Bagan, P. Ball, V.M. Braun and P. Gosdzinsky, Nucl. Phys. B432 (1994) 3.
- [9] E. Bagan, P. Ball, B. Fiol and P. Gosdzinsky, Phys. Lett. B351 (1995) 546.
- [10] E. Bagan, P. Ball, V.M. Braun and P. Gosdzinsky, Phys. Lett. B342 (1995) 362; Erratum *ibid* B374 (1996) 363.
- [11] G. Altarelli and S. Petrarca, Phys. Lett. B261 (1991) 303.
- [12] M. Neubert, hep-ph/9605256, to appear in the proceedings of the *10th Les Rencontres de Physique de la Vallee d'Aoste*, La Thuile, 1996.
- [13] G. Buchalla, I. Dunietz and H. Yamamoto, Phys. Lett. B364 (1995) 188.
- [14] I. Dunietz, J. Incandela, F.D. Snider and H. Yamamoto, hep-ph/9612421.
- [15] ALEPH coll., EPS-404, contribution to the *Int. Europhysics Conf. on High Energy Physics*, Brussels, 1995.
 P. Abreu *et al.* (DELPHI), Z. Phys. C66 (1995) 323.
 M. Acciarri *et al.* (L3) Z. Phys. C71 (1996) 379.
 R. Akers *et al.* (OPAL), Z. Phys. C60 (1993) 199.
- [16] M. Neubert, hep-ph/9610385, to appear in the proceedings of the *20th John Hopkins Workshop on Current Problems in Particle Theory*, Heidelberg, 1996.
- [17] S. Bertolini, F. Borzumati and A. Masiero, Nucl. Phys. B294 (1987) 321.
 A.L. Kagan, Phys. Rev. D51 (1995) 6196.
 M. Ciuchini, E. Gabrielli and G.F. Giudice, Phys. Lett. B388 (1996) 353.
 A.L. Kagan and J. Rathsman, hep-ph/9701300.
- [18] W.F. Palmer and B. Stech, Phys. Rev. D48 (1993) 4174.
- [19] R. Fleischer, Z. Phys. C 58 (1993) 483.
- [20] G. Altarelli, G. Curci, G. Martinelli and S. Petrarca, Nucl. Phys. B187 (1981) 461.
- [21] W. A. Bardeen, A. J. Buras, D. W. Duke and T. Muta, Phys. Rev. D18 (1978) 3998.
- [22] A.F. Falk, Z. Ligeti, M. Neubert and Y. Nir, Phys. Lett. B326 (1994) 145.
- [23] G. Buchalla, Nucl. Phys. B391 (1993) 501.
- [24] A. J. Buras and R. Fleischer, Phys. Lett. B341 (1995) 379.

- [25] M. Ciuchini, E. Franco, G. Martinelli and L. Silvestrini, hep-ph/9703353.
- [26] M.A. Shifman, A.I. Vainshtein and V.I. Zakharov, Phys. Rev. D18 (1978) 2583 ; Erratum *ibid.* D19 (1979) 2815.
B. Grinstein, R. Springer and M.B. Wise, Phys. Lett. B202 (1988) 138; Nucl. Phys. B339 (1990) 269.
- [27] M. Ciuchini, E. Franco, G. Martinelli, L. Reina and L. Silvestrini, Phys. Lett. B316 (1993) 127.
M. Ciuchini, E. Franco, L. Reina and L. Silvestrini, Nucl. Phys. B421 (1994) 41.
M. Ciuchini, E. Franco, G. Martinelli, L. Reina and L. Silvestrini, Phys. Lett. B334 (1994) 137.
- [28] A. J. Buras, M. Jamin, M. E. Lautenbacher and P. H. Weisz,
Nucl. Phys. B370 (1992) 69; Addendum *ibid* B375 (1992) 501.
A. J. Buras, M. Jamin, M. E. Lautenbacher and P. H. Weisz,
Nucl. Phys. B400 (1993) 37.
- [29] S. Bethke, hep-ex/9609014, talk given at the *International Euroconference on Quantum Chromodynamics (QCD 96)*, Montpellier, 1996.
- [30] S. Herrlich and U. Nierste, Nucl. Phys. B455 (1995) 39.
S. Herrlich and U. Nierste, Nucl. Phys. B476 (1996) 27.
- [31] H. Simma, G. Eilam and D. Wyler, Nucl. Phys. B352 (1991) 367.
- [32] Y. Nir, Phys. Lett. B221 (1989) 184.
- [33] I. Bigi, M. Shifman and N. Uraltsev, hep-ph/9703290.
- [34] M. Artuso, Nucl. Instrum. Meth. A384 (1996) 39.
- [35] S. Herrlich and U. Nierste, Phys. Rev. D52 (1995) 6505.
U. Nierste, hep-ph/9609310, talk given at the *Workshop on K physics*, Orsay, May/June 1996.